Title
Asian chemical outflow to the Pacific in late spring observed during the PEACE-B aircraft mission

Journal
Journal of Geophysical Research, 109(D23)

ISSN
0148-0227

Authors
Oshima, N
Koike, M
Nakamura, H
et al.

Publication Date
2004-12-16

DOI
10.1029/2004jd004976

Asian chemical outflow to the Pacific in late spring observed during the PEACE-B aircraft mission

N. Oshima,[1] M. Koike,[1] H. Nakamura,[1] Y. Kondo,[2] N. Takegawa,[2] Y. Miyazaki,[2] D. R. Blake,[3] T. Shirai,[4,5] K. Kita,[6] S. Kawakami,[4] and T. Ogawa[4]

Received 1 May 2004; revised 30 August 2004; accepted 7 October 2004; published 8 December 2004.

[1] The Pacific Exploration of Asian Continental Emission phase B (PEACE-B) aircraft mission was conducted over the western Pacific during April–May 2002. During several flights, large enhancements of CO greater than 200 parts per billion by volume (ppbv) were observed at altitudes between 5 and 10 km. In this paper, we describe vertical transport mechanisms over east Asia that were responsible for these enhancements, using the European Centre for Medium-Range Weather Forecasts (ECMWF) meteorological data and infrared cloud data obtained by the Geostationary Meteorological Satellite (GMS)-5. A case study for the highest CO event shows that it was likely due to vertical transport of pollutants caused by deep cumulus convection along a quasi-stationary frontal zone, which was formed over central China (around the Yangtze River at 30°N). In the mean meteorological field during the PEACE-B period, the warm, moist low-level southerlies converged into the frontal zone, sustaining cross-frontal temperature and moisture contrasts. Along the frontal zone, the mean vertical motion was distinctively upward, and a subtropical jet aloft was found to transport uplifted air parcels efficiently into the western Pacific. In this study, criteria to identify deep convection are defined using both the ECMWF and GMS data. The results show that convective activity, which was generally high below the subtropical jet, played an important role in producing updrafts over central China. The convective transport resulted mainly from a limited number of episodes, each of which followed the development of a weak cyclonic disturbance. Back trajectories of air parcels sampled at altitudes between 4 and 13 km on board the aircraft during PEACE-B show that among the air parcels originating from the 800-hPa level or below, 69% were likely to have undergone convective uplifting. In addition to convection, sloping isentropes often observed along the quasi-stationary jet axis yielded persistent slow quasi-adiabatic uplifting of air over the Far East, which was occasionally intensified with a classical warm conveyor belt (WCB) airstream on the passage of migratory cyclonic disturbances. Meteorological conditions during PEACE-B were thus favorable for the uplifting of boundary layer air influenced by anthropogenic emissions over central China. These results are consistent with the relatively high levels of Halon 1211 (CF_2ClBr), a good tracer of Chinese anthropogenic emissions, observed in the air parcels that were likely uplifted in the frontal zone. *INDEX TERMS:* 0368 Atmospheric Composition and Structure: Troposphere—constituent transport and chemistry; 0365 Atmospheric Composition and Structure: Troposphere—composition and chemistry; 0345 Atmospheric Composition and Structure: Pollution—urban and regional (0305); *KEYWORDS:* transport, convection, chemical outflow

Citation: Oshima, N., et al. (2004), Asian chemical outflow to the Pacific in late spring observed during the PEACE-B aircraft mission, *J. Geophys. Res.*, *109*, D23S05, doi:10.1029/2004JD004976.

1. Introduction

[2] An understanding of the processes controlling the vertical transport of air from the planetary boundary layer (PBL) to the free troposphere (FT) is critically important in order to evaluate regional- and intercontinental-scale impacts of anthropogenic emissions and biomass burning on the atmospheric environment and climate. In the FT, the chemical destruction rate and wet removal rate tend to be lower than in the PBL, while the horizontal wind speed is

[1]Department of Earth and Planetary Science, Graduate School of Science, University of Tokyo, Tokyo, Japan.
[2]Research Center for Advanced Science and Technology, University of Tokyo, Tokyo, Japan.
[3]Department of Chemistry, University of California, Irvine, California, USA.
[4]Earth Observation Research and Application Center, Japan Aerospace Exploration Agency, Tokyo, Japan.
[5]Now at National Institute for Environmental Studies, Ibaraki, Japan.
[6]Department of Environmental Sciences, Faculty of Science, Ibaraki University, Ibaraki, Japan.

0148-0227/04/2004JD004976

greater. As a consequence, once pollutants emitted at the ground surface are transported into the FT, they will have a greater chance of being transported over long distances, causing wider-scale pollution problems.

[3] In the extratropics, two types of uplifting processes of air have been recognized as important: cumulus convection and the warm conveyor belt (WCB). On the basis of the vertical profiles of various species over land in summer, deep convection has been found to be an important venting mechanism of pollutants from the PBL into the FT [*Dickerson et al.*, 1987; *Pickering et al.*, 1992]. As is also well known [e.g., *Carlson*, 1991], a WCB is a poleward airstream rising gradually ahead of a surface cold front associated with a synoptic-scale cyclone system. Since the airstream is not associated with convective precipitation, except around (frontal) rainbands, the diabatic heating rate due to latent heat release is, in general, relatively low along a WCB. Therefore an air parcel tends to stay approximately on the same isentrope as it moves poleward over some distance along a WCB, which we will henceforth refer to as ''quasi-adiabatic'' motion. The ascent rate of an air parcel along a WCB is thus generally lower than that associated with cumulus convection. Although the WCB airstream itself has been known to meteorologists for some time, its importance as an efficient mechanism for the transport of surface pollutants was not recognized until recent aircraft measurements were made available [*Brunner et al.*, 1998; *Stohl and Trickl*, 1999; *Cooper et al.*, 2001; *Bethan et al.*, 1998; *Kowol-Santen et al.*, 2001].

[4] The relative importance of these two venting processes at various locations and seasons has been studied using modeling and trajectory analyses. *Stohl* [2001] presented seasonal statistics of airstreams over the Northern Hemisphere for a particular year based on a large number of trajectory calculations, to show that WCBs originate most frequently over warm water pools off the eastern seaboards of North America and Asia. He also showed that WCB mass fluxes peak in winter and are at a minimum in summer. These seasonal and geographical characteristics of WCBs have been confirmed in the 15-year climatology of trajectories of *Eckhardt et al.* [2004], where WCBs over the North Pacific appear eight times more frequently in winter than in summer. Using a mesoscale model, *Hov and Flatøy* [1997] showed that convective uplifting is generally much stronger than a synoptic-scale ascent over summertime Europe under the influence of a high-pressure system, while the contribution from convection is substantially smaller in fall. *Brunner et al.* [1998] attributed the high-NO_x plumes observed in the upper troposphere over the Atlantic and other regions to convective activity over the continent (vertical transport of pollution and lightning NO production) in summer and vertical transport within frontal systems (WCBs and others) in other seasons. *Cotton et al.* [1995] concluded that on a global-annual basis, upward motion of air caused by cyclones (WCBs and others) had the largest PBL mass flux of all cloud venting systems, followed by mesoscale convective systems.

[5] It has also been recognized that the broad zone of a gently ascending WCB often contains organized rainbands with locally enhanced ascent associated with convective activity [*Browning*, 1990; *Esler et al.*, 2003]. The convective transport associated with frontal activity increases an upward mass flux by 10–20% [*Donnell et al.*, 2001]. Consequently, it is difficult to quantitatively separate observed upward mass transport associated with a frontal passage into contributions from ''advective'' (WCB and others) and convective upward motion.

[6] Because of the rapid economic growth and industrialization in the People's Republic of China and other Asian countries, understanding of vertical transport mechanisms in east and Southeast Asia is especially important. To investigate Asian chemical outflow, several aircraft missions have been conducted over the western Pacific in winter and spring, such as the NASA Pacific Exploratory Mission-West (PEM-West B) conducted in February–March 1994 and the NASA Transport and Chemical Evolution over the Pacific (TRACE-P) mission conducted during February–April 2001. From the PEM-West B study, *Xiao et al.* [1997] showed that the passage of cold fronts over east Asia caused continental outflows of sulfur and dust into the western Pacific. *Bey et al.* [2001] showed that the lower tropospheric convergence over central and eastern China enhanced an upward flux of CO into the lower FT. They concluded that this upward motion associated with episodic frontal lifting ahead of eastward moving cold fronts and the subsequent westerly transport were the primary processes responsible for the export of both anthropogenic and biomass burning pollution from Asia during PEM-West B. *Liu et al.* [2003] showed that the large-scale convergence over central and eastern China was also observed during March in other years and that frontal lifting (largely due to WCBs) was the major process for chemical outflows also during TRACE-P. They proposed orographic uplifting as another major process responsible for the lifting of polluted air to the FT. They also showed that deep cumulus convection was more important in driving the export of biomass burning effluents from Southeast Asia. *Hannan et al.* [2003] demonstrated that airstreams observed around synoptic-scale fronts responsible for venting the PBL air mass differ considerably from those described in classical conceptual models or in the recent literature. Analyzing trajectories of air parcels sampled in the FT during TRACE-P, *Miyazaki et al.* [2003] showed that most of the uplifted air parcels had been influenced either by WCBs associated with midlatitude cyclones or convective activity associated with stationary fronts over southeast China. As an important feature of these transport mechanisms from east Asia, other observations [*Jaffe et al.*, 1999] and modeling studies [*Yienger et al.*, 2000; *Wild and Akimoto*, 2001] have also shown that a significant portion of the outflow of Asian pollution was caused by a limited number of episodes rather than by persistent circulation.

[7] The Pacific Exploration of Asian Continental Emission phase B (PEACE-B) aircraft mission was conducted over the western Pacific between 21 April and 16 May 2002, within the framework of the atmospheric chemistry project of the Earth Observation Research Center (EORC) of the Japan Aerospace Exploration Agency (JAXA). In total, 12 flights were conducted over the Japan Sea, East China Sea, and Pacific Ocean using a Gulfstream II (G-II) aircraft (Figure 1). The major objectives of the PEACE-B mission are to study transport processes and chemical features of the continental outflow over the western Pacific, especially from east Asia, in late spring. The PEACE-A

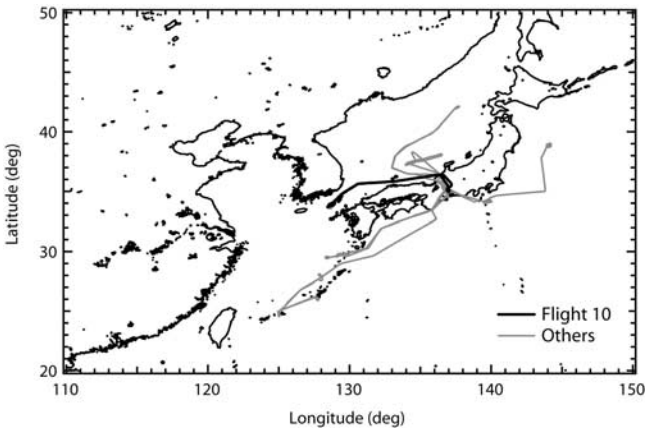

Figure 1. Flight tracks for the G-II aircraft during the PEACE-B aircraft mission (21 April to 16 May 2002).

aircraft mission was conducted in January 2002 with the same instrumentation as in PEACE-B. A detailed description of the PEACE-A and PEACE-B missions is given by *Kondo et al.* [2004]. During the PEACE-B period, the Intercontinental Transport and Chemical Transformation (ITCT 2K2) mission was conducted simultaneously over the west coast of the United States to study intercontinental transport of Asian pollutants across the Pacific [*Parrish et al.*, 2004].

[8] In this paper, vertical transport mechanisms over east Asia during the PEACE-B period are described. In particular, we focus on the role of deep cumulus convection over central China, which was likely to bring pollutants in that region effectively into the FT. Chemical characteristics of uplifted air parcels are also presented using the PEACE-B data.

2. Meteorological Conditions During the PEACE-B Period

[9] Mean meteorological fields during the PEACE-B period (10 April through 20 May 2002) are shown in Figures 2a–2d, based on operational analyses of the European Centre for Medium-Range Weather Forecasts (ECMWF) data. The 6-hourly data are available on a regular grid with a resolution of 1° both in latitude and longitude at each of the 12 standard pressure levels (1000–70 hPa). The low-level circulation over the Far East during the PEACE-B period was characterized by mean southerlies over southern China, the Indochina Peninsula, and the East China Sea, seemingly associated with a predominant anticyclone persistent over the central Pacific (Figure 2a). Part of the southerly flow extended northeastward, merging over Japan into the prevailing westerlies from the continent. The rest of the southerlies were strongly converging into a quasi-stationary frontal zone that extended more or less zonally along the Yangtze River, as denoted by a heavy solid line in Figures 2a and 2b (we call the region around this frontal zone the "central China region" hereafter). The frontal zone was marked by a sharp meridional gradient in lower tropospheric equivalent potential temperature (θ_e) (Figure 2b). In fact, a stationary front was often analyzed in this region during the PEACE-B period, and in many of such occasions a weak cyclonic disturbance developed along the front and then migrated eastward. Along the frontal zone, a distinct mean updraft was observed in the midtroposphere (Figure 2c). The mean midtropospheric upward motion was also pronounced in the Assam region (northeastern India) and in the northern portion of the Indochina Peninsula, where the low-level southerlies or southwesterlies hit the southern slopes of major mountain ranges.

[10] The mean upper tropospheric circulation over the Far East during the PEACE-B period was characterized by a double-jet structure over the continent. The two branches of the westerlies were confluent downstream to form a jet core region over Japan (Figure 2d). The surface frontal zone and associated midtropospheric ascent were located below the mean southwesterlies that constitute the subtropical branch of the double-jet structure. The subtropical southwesterly jet accompanied a persistent upper level pressure trough above the southeastern portion of the Tibetan Plateau and a persistent pressure ridge over the western Pacific. These large-scale geographically fixed trough and ridge are components of planetary waves that must be generated in response to persistent forcing at the surface throughout most of the PEACE-B period. Downstream of the trough, the associated cyclonic vorticity advection by the mean westerlies must be balanced with the anticyclonic vorticity generation due to the midtropospheric ascent and associated divergence aloft. Hence the close association between the mean updraft in the surface frontal zone around the Yangtze River (central China) and the southwesterly jet aloft is dynamically consistent from the viewpoint of vorticity balance. The pronounced mean ascent in the frontal zone was associated with enhanced cumulus convection in this region, marked as a band of outgoing longwave radiation (OLR) minima (Figure 2c). The moisture transport by the low-level southerlies into the frontal zone (Figure 2b) acts to sustain the convective activity. As shown later, the convective activity and updraft tended to be enhanced when a cyclonic disturbance developed. The mean circulation pattern characterized by the low-level southerlies over southern China, convective activity in the frontal zone to the north, and the subtropical southerly jet aloft appear to constitute conditions favorable for the transport of pollutants emitted by industrial activity in the coastal region of southern China into the PEACE-B study area.

[11] Five-day kinematic back trajectories of air parcels sampled from the G-II research aircraft at altitudes between 4 and 13 km during PEACE-B were calculated using the ECMWF data. Figures 3a and 3b show the trajectories of air parcels that originated from below the 800-hPa level in the east Asian region (10°–50°N, 80°–150°E). In Figure 3b, changes in potential temperature along the trajectories are indicated with colors, superimposed on the mean distribution of potential temperature along the axis of the upper level subtropical southwesterly jet (in a cross section along the heavy solid line in Figure 2d between 25°N, 100°E and 40°N, 145°E) during the PEACE-B period. Most of the air parcels sampled were transported northeastward by the southwesterlies along the subtropical jet (Figure 3a). Two types of upward air motion are evident in the cross section of the trajectories shown in Figure 3b. Air parcels in the first category underwent rapid uplifting

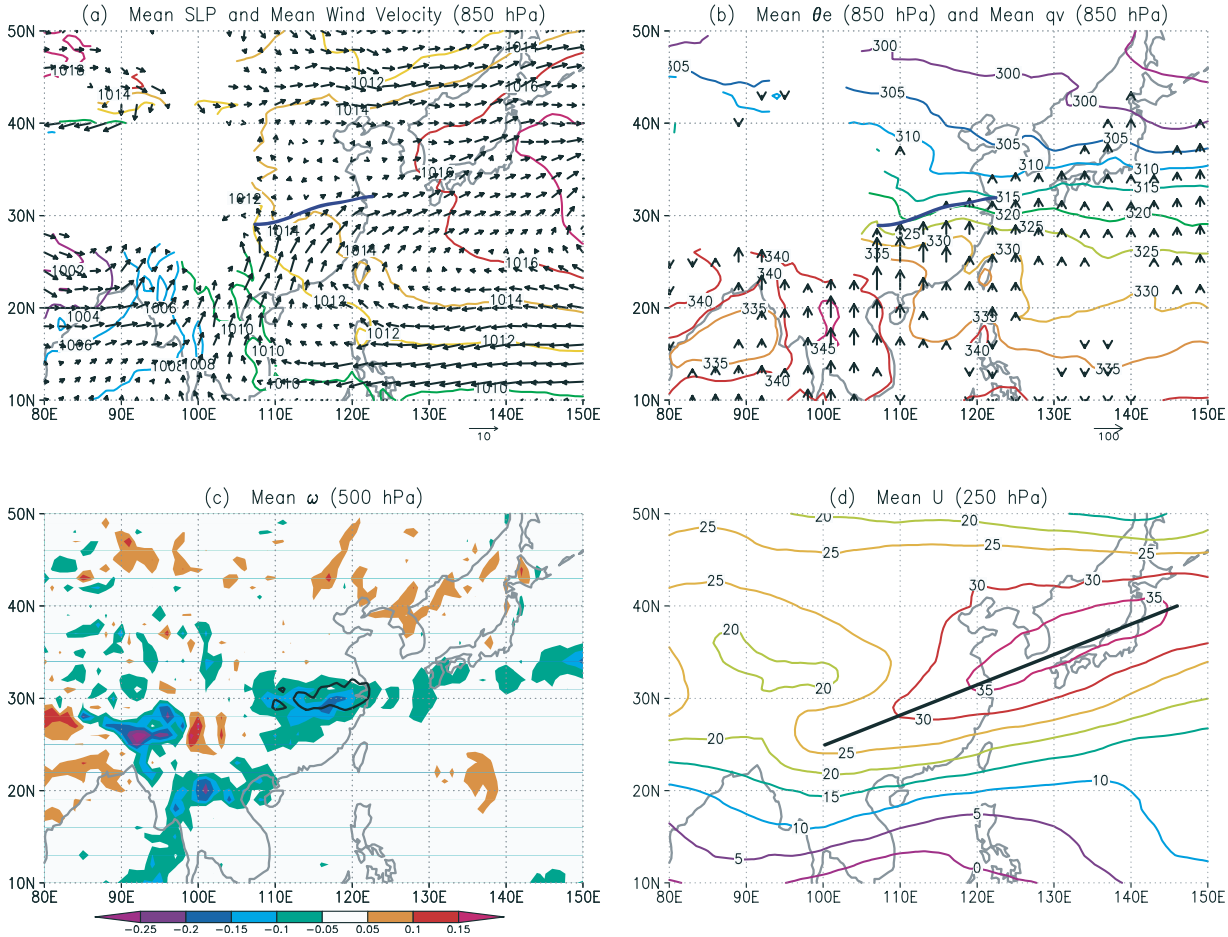

Figure 2. Mean meteorological fields over the Far East during the PEACE-B period (10 April to 20 May 2002). (a) Mean sea-level pressure (hPa, contours) and mean horizontal winds at the 850-hPa level (m s^{-1}, vectors with scaling near the lower right corner). The heavy solid line denotes the location of the quasi-stationary frontal zone over central China described in the text (section 2). Regions without data correspond to those of high-altitude mountains. (b) Mean equivalent potential temperature θ_e (K, contours) and total meridional moisture transport (qv values in vector form with scaling near the lower right corner) at the 850-hPa level (m s^{-1} g Kg^{-1}). qv vectors with magnitudes greater than 10 m s^{-1} g Kg^{-1} are plotted. (c) Mean vertical wind velocity (ω-velocity) at the 500-hPa level (Pa s^{-1}, filled contours) and regions where the mean T_{BB} (equivalent black body temperature derived from IR image obtained by the GMS) was lower than 261 K (regions encircled by black solid lines). The low-T_{BB} regions likely due to the cold surfaces, such as high-altitude mountains (Tibetan and Mongolian Plateaus), are not shown. (d) Mean westerly wind speed at the 250-hPa level (m s^{-1}). The heavy solid line denotes the mean axis of the subtropical southwesterly jet.

across isentropes, which must be due to latent heat release associated with convective precipitation. Many of these updraft trajectories were located over the central China region in accordance with deep convection enhanced over this region as seen in OLR minima described above (Figure 2c). Limitations in resolving subgrid-scale convection by grid-scale trajectory calculations are discussed in section 3.1, and detailed descriptions on the identification of deep convection are given in section 3.2. Air parcels in the second category underwent gradual uplifting associated with their quasi-adiabatic motion along the subtropical jet stream. Interestingly, some air parcels likely experienced those two upward transport processes in sequence, i.e., convective uplifting followed by quasi-adiabatic gradual ascending motion and vice versa.

[12] One may consider that slowly ascending airstreams of the second category were associated with WCBs. In fact, as discussed in section 3.3, this was likely the case on particular occasions during the PEACE-B period when weak cyclonic disturbances migrated along the frontal zone. Nevertheless, the following cautionary remarks must be made. First, the slope of isentropic surfaces along the subtropical jet observed in the time mean field (Figure 3b) was dynamically consistent with mean low-level southerlies that decreased with increasing altitude, indicating low-level frontogenesis due to mean warm advection. Therefore gradual upward air motion along the subtropical jet could occur even without any migratory disturbances, and thus the ascending airstreams could be fixed geographically, in contrast to those associated with classical WCBs. Second,

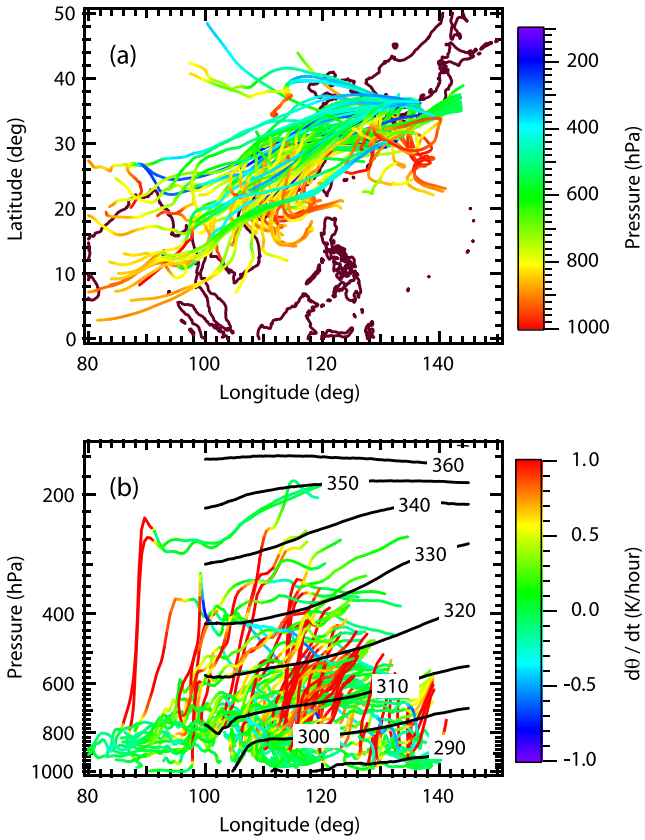

Figure 3. Five-day back trajectories of air parcels that originated from below the 800-hPa level in the east Asian region (10°–50°N, 80°–150°E). (a) Their horizontal distribution. Colors indicate atmospheric pressure along the trajectories. (b) Their distribution in a longitude-pressure cross section. Changes in potential temperature along the trajectories are indicated with colors. Black solid lines show the mean distribution of potential temperature along the axis of the upper level subtropical southwesterly jet (in a cross section along the heavy solid line in Figure 2d between 25°N, 100°E and 40°N, 145°E) during the PEACE-B period.

the geographically fixed nature of an ascending airstream associated with such a persistent localized jet as observed in the PEACE-B period will remain, even if large-scale quasi-stationary fluctuations are embedded in association with group-velocity propagation of Rossby waves whose timescales are longer than those of migratory synoptic-scale systems. As shown later, we observed an enhancement of the planetary-wave pattern during an incident of stationary Rossby wave propagation in the middle of the PEACE-B period. The steady and geographically fixed nature of slowly ascending airstreams associated with the frontogenetic subtropical jet observed in the PEACE-B period is distinct from the more transient nature of slowly ascending airstreams associated with classical WCBs. Therefore the "quasi-adiabatic" trajectories indicated in Figure 3b cannot necessarily be interpreted in the framework of the classical WCB airstreams associated with migratory cyclones. Rather, as described later in section 3.3, cyclonic disturbances that migrated along the frontal zone acted as a trigger for the enhancement of both deep convection and quasi-adiabatic upward motion through the intensification of the low-level southerlies. While the enhancement of quasi-adiabatic ascent is essentially the same as in the development of a classical WCB, the enhancement of cumulus convection is a distinct characteristic of cyclogenesis in a subtropical frontal zone, including a Baiu (Meiyu) front, under an abundant moisture supply with modest mean-flow baroclinicity in the warm season. Consequently, air parcels uplifted by these two processes were found together around the frontal zone, as suggested in Figure 3b.

3. Transport Processes of Convective Outflow

3.1. A Case Study of Convective Outflow

[13] In this study, we used CO as a tracer to identify air parcels that had been influenced by anthropogenic emissions and biomass burning followed by vertical transport from the PBL. Figure 4 shows vertical profiles of CO mixing ratio using all of the data obtained during the PEACE-B aircraft mission. Enhancements of CO were observed in the FT during several flights. Pronounced enhancements with CO concentrations greater than 200 parts per billion by volume (ppbv) were observed between 5 and 10 km during flight 10, on 14 May 2002. We focused on this flight to study detailed mechanisms of the vertical transport of air parcels over east Asia. The flight track and the observed CO concentrations are shown in Figures 1, 5a, and 5b. The enhancements of CO (greater than 200 ppbv) in the FT were observed at longitudes between 128°E and 138°E, suggesting that high-CO air spread zonally over 1000 km in distance. In Figures 5a and 5b, 5-day back trajectories of air parcels, in which CO mixing ratios were greater than 200 ppbv, are shown for the highest CO event. The trajectories indicate that these high-CO air parcels were located in the lower troposphere (800-hPa level or below) over central China 24–30 hours prior to the measurements. They then underwent rapid uplifting from the 800-hPa to 500-hPa level within the following 10 hours over the central China region.

[14] Finally, the uplifted air parcels were transported horizontally toward the western Pacific by the midtropospheric westerlies (~400–500-hPa levels) along the subtropical jet until they were sampled by the G-II aircraft. As suggested by forward trajectories (Figure 5c), part of these air parcels could be transported further by the westerlies to North America within the following 5 days. Although these particular air parcels were not sampled over the west coast of the United States during the ITCT mission, uplifted air parcels influenced by anthropogenic emission over east Asia can cross the Pacific within a week and can have an impact on the atmospheric environment over the United States.

[15] Meteorological fields during the period when the air parcels were rapidly uplifted (0600 UTC on 13 May 2002) are shown in Figures 6a–6c. In association with a weak cyclone at the surface, the warm, moist southerlies in the lower troposphere intensified over southern China (Figure 6a), converging into a front extending between 20°N, 100°E and 30°N, 115°E. In good agreement with the enhanced low-level convergence, the midtropospheric upward motion was also enhanced along the front

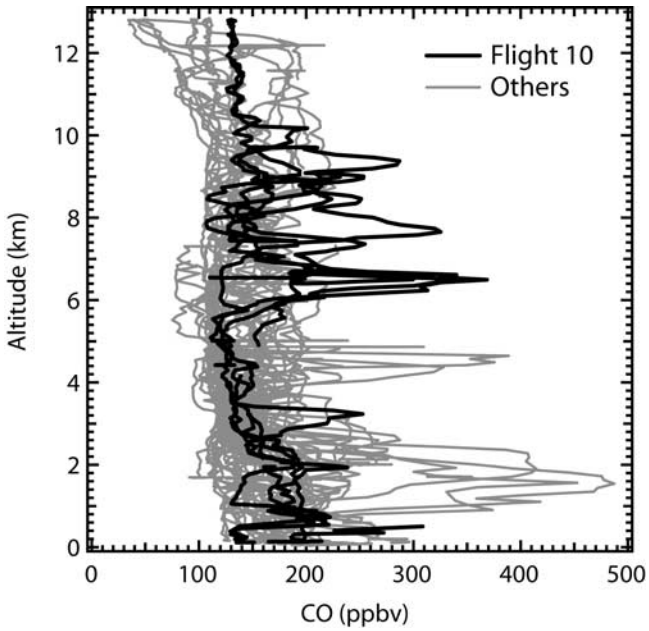

Figure 4. Vertical profiles of CO mixing ratio (10-s mean data) measured during the PEACE-B period. The black and gray lines denote CO mixing ratios sampled during flight 10 (14 May 2002) and the other flights, respectively.

(Figure 6b), with a maximum velocity in the vicinity of the surface cyclone around 30°N, 112°E. An infrared (IR) image obtained by the Geostationary Meteorological Satellite (GMS)-5 shown in Figure 6d clearly indicates the presence of deep convective clouds with equivalent black body temperatures (T_{BB}s) below 220 K (or, equivalently, cloud top altitudes higher than 10 km) along the front associated with the pronounced ascent. Therefore the rapid uplifting of CO-rich air parcels into the FT as revealed in the trajectory analysis was quite likely due to deep convection in the quasi-stationary frontal zone over central China. Changes in potential temperature (>1 K/hour) along the trajectories are also consistent with rapid diabatic uplifting in the vicinity of the mesoscale convective activity (see Figure 3b).

[16] As in the mean fields (Figures 2a–2d), the surface front and associated upward motion in this particular period were located below the upper tropospheric subtropical jet (Figures 6a–6c). The collocation of the enhanced updraft with the subtropical jet was favorable for the rapid uplifting and subsequent fast horizontal transport toward the western Pacific of air parcels situated initially near the surface over central China.

[17] We note that since individual convection events are mesoscale phenomena, there must be certain limitations in representing convective air parcel motion based on the 6-hourly 100-km-grid-size data. For example, during the Stratosphere-Troposphere Experiment: Radiation, Aerosol, and Ozone (STERAO)–Deep Convection experiment, convective activity typically consisted of cells with horizontal scales of only 15–20 km [*Dye et al.*, 2000], through which it took approximately only 10 min for air parcels to ascend from 2.5 km above the ground surface to the anvil [*Skamarock et al.*, 2000]. In the gridded ECMWF data, this kind of subgrid-scale convection is taken into account implicitly in a more or less consistent manner so that grid-scale vertical motion and associated meteorological variables have been evaluated with the parameterized effects of diabatic heating associated with convective precipitation. Analyzed vertical velocity (and therefore mass flux) for convective grid boxes is thus systematically higher than that for nonconvective (e.g., WCB) grid boxes. In fact, *Rasch et al.* [1997] showed that tracer transport calculations with "off-line models" on the basis of 6-hourly gridded

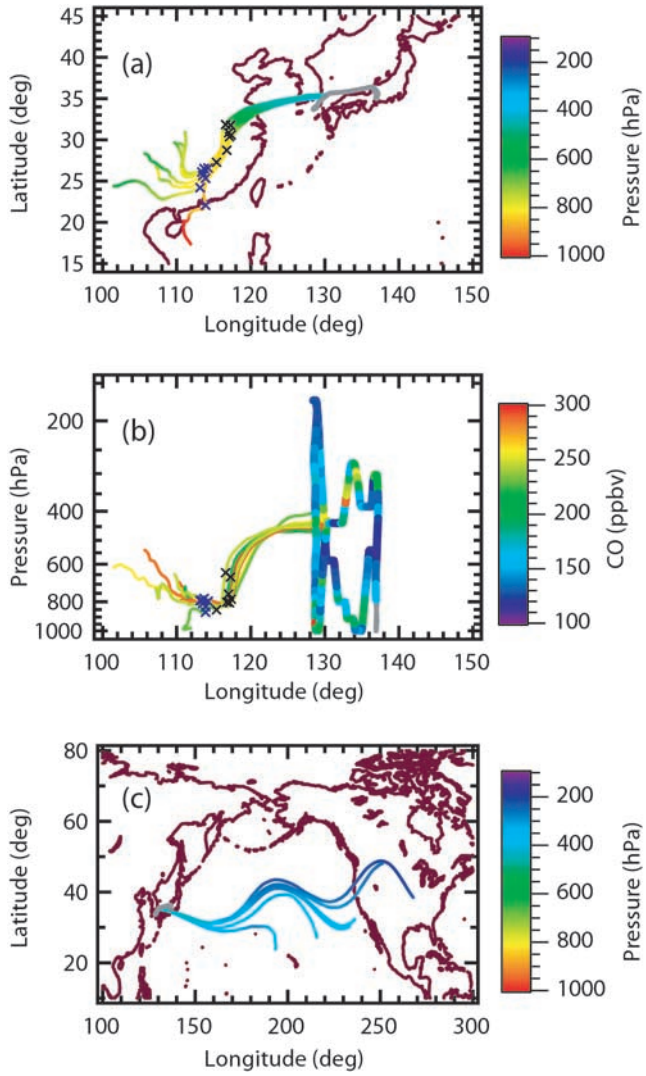

Figure 5. (a) Five-day back trajectories for air parcels in which the highest CO mixing ratios were observed, during flight 10 (0600 UTC on 14 May 2002). The trajectories were calculated from G-II aircraft locations every 5 min. The colors of the trajectories indicate atmospheric pressure along the trajectories. Black and blue crosses denote the locations of air parcels 24 and 48 hours prior to the measurements, respectively. The gray line denotes the flight track. (b) Vertical profiles of the trajectories on the longitude-pressure cross section (thin color lines) and the flight track (thick color lines). The colors of both the trajectories and flight track indicate CO mixing ratios at individual sampling points. (c) Five-day forward trajectories for the same air parcels.

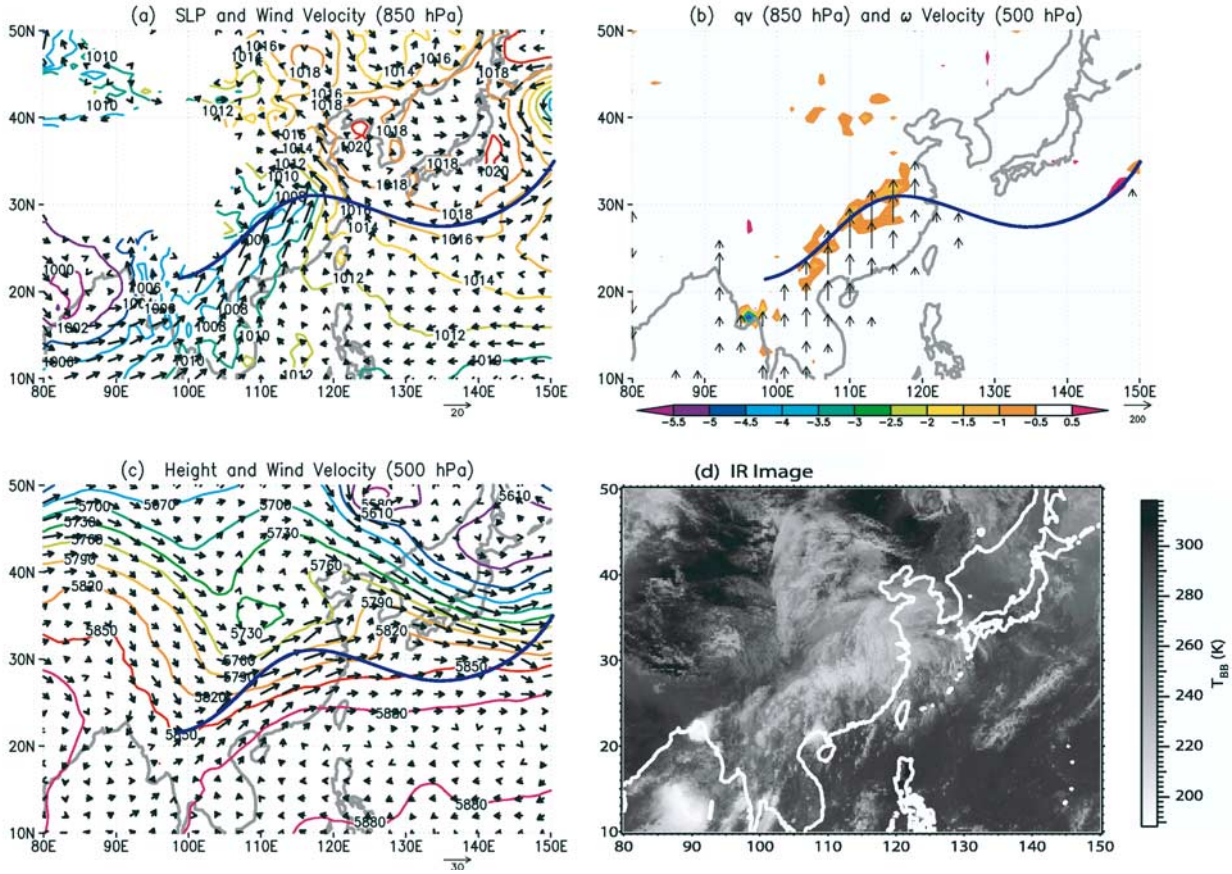

Figure 6. Meteorological fields and an IR image from the GMS satellite on the day when air parcels in which the highest CO was observed during flight 10 were uplifted over central China (0600 UTC on 13 May 2002). (a) Sea-level pressure (hPa, contours) and horizontal winds at the 850-hPa level (m s^{-1}, vectors with scaling near the lower right corner). The heavy solid line denotes the approximate locations of surface fronts. (b) Vertical wind velocity (ω-velocity) at the 500-hPa level (Pa s^{-1}, filled contours) and meridional moisture transport (in vector form with scaling near the lower right corner) at the 850-hPa level (m s^{-1} g Kg^{-1}). (c) As in Figure 6a, but for horizontal winds (m s^{-1}, vectors) and geopotential height (contours) at the 500-hPa level. (d) IR cloud image obtained by the GMS. The scaling for T_{BB} (K) is given on the right-hand side.

circulation fields analyzed operationally can be nearly as accurate as those based on general circulation models (GCMs). In these "on-line models," grid-scale flows and parameterized subgrid-scale mass fluxes are updated at each time step for evaluation of tracer transport. Although trajectories of individual air parcels influenced by convection cannot be accurately reproduced by our calculations, a cluster of calculated trajectories showing rapid uplifting across isentropes (Figure 3b) should reflect an aggregate effect of convective transport over central China. The vertical transport time based on our evaluation (such as 10 hours, shown in Figure 5b) should therefore not be regarded as that representing fast mesoscale updraft in convective cells. Rather it should more or less represent the mean ascent rate within a convective grid box that tends to be substantially larger than that for nonconvective grid boxes.

3.2. Definition of Convection and Its Spatial Distribution

[18] In the case study presented in section 3.1, deep convection was considered responsible for the vertical transport because of the good agreement in the occurrence time and location between the enhanced upward motion of air parcels and high-altitude clouds. In this section, criteria to identify deep convection are defined by expanding this idea, and a spatial distribution of the occurrence probability of convective activity during the PEACE-B period is presented.

[19] It is difficult to unambiguously distinguish between vertical transport processes associated with cumulus convection and WCBs using only the ECMWF meteorological data. It is also difficult to unambiguously distinguish between deep cumulus and cirrus clouds based solely on the GMS IR image (T_{BB}) data. In this study, these two (ECMWF and GMS) independent data sets were combined to identify deep convection. The criteria for deep cumulus convection were defined as follows: (1) cloud top height (based on the GMS T_{BB}) higher than 10 km, (2) negative (i.e., upward) 500-hPa ω-velocity stronger than 0.5 Pa/s in magnitude, (3) 850-hPa relative humidity greater than 80%, and (4) 850-hPa θ_e higher than 310 K. The last two criteria were adopted to ensure a sufficient moisture supply in the

lower troposphere for cumulus convection. At each time step (every 3 hours), these criteria were applied to the hourly T_{BB}data and the time-interpolated ECMWF data in each grid box (1° × 1°), and an occurrence of deep convection was identified when all of these criteria were satisfied. Note that these criteria were chosen rather subjectively, and the threshold values should be changed depending on the resolution of meteorological data, geographical location, and/or season. The number of convection events identified by these criteria is especially sensitive to a particular choice of the threshold value for ω-velocity. On the basis of the ECMWF data (with 1° × 1° resolution), *Miyazaki et al.* [2003] estimated the mean trajectory-based (Lagrangian) ascent rate associated with cumulus convection and WCBs to be 4.7 ± 2.5 and 2.3 ± 1.1 km/24 hours, respectively, for the events identified over the western Pacific during the TRACE-P period. These ascent rates correspond to 500-hPa ω-velocities of approximately −0.37 and −0.18 Pa/s, respectively. *Stohl* [2001] regarded trajectories as being associated with WCBs if they ascended at least 8 km within 48 hours from their starting levels between 0.5 and 1.5 km above the surface (and, in addition, if they traveled to the northeast at least 5° latitude and 10° longitude). His criterion corresponds to a midtropospheric ω-velocity of approximately −0.32 Pa/s. *Eckhardt et al.* [2004] also used similar criteria. Thus our particular choice of −0.5 Pa/s as a criterion for convective activity seems appropriate for discriminating a convective updraft from a more gradual ascent due to a WCB. Note that the criteria adopted in this study require no calculation of air parcel trajectories. In this sense, they may be considered as Eulerian-type criteria that have a great computational advantage. Though rather subjective, the aforementioned criteria were applied to the gridded data sets to identify convective activity at every 1° × 1° grid box within the entire Far East at 3-hour intervals throughout the 40-day PEACE-B period. As noted in section 3.1, our identification of air parcel motion possibly influenced by convective activity based on the 6-hourly 100-km-grid-size data is subject to various limitations. Nevertheless, as already discussed, the use of ω-velocity based on the ECMWF analyses is reasonable to at least identify the occurrence of convective transport.

[20] The occurrence probability (time fraction) of convective activity in each grid box defined with the above criteria over east Asia during the PEACE-B period is shown in Figure 7 (color-coded). Deep convection was found to occur frequently along the quasi-stationary frontal zone over central China, as suggested by rapidly ascending trajectories of air parcels sampled in the PEACE-B mission (Figure 3b). Frequent occurrence of deep convection was also found off the east coast of Japan and over western Japan, probably associated with frontal or cyclone activity along the strong westerly jet. In addition, frequent convective activity in some portions of the Indochina Peninsula and northeastern India was likely associated with premonsoonal precipitation. All of these regions correspond well to those where the mean ascent was significant (Figure 2c). Although the specific values of the occurrence probability depend on a particular choice of the threshold values used for the convective activity definition, the spatial distribution of the probability should be more robust. A comparison with the results using trajectory-based (Lagrangian) criteria adopted in earlier studies is given later in section 3.5.

[21] The frequent occurrence of convective activity over the central China region (Figure 7) suggests that convective transport likely played an important role in uplifting air masses influenced by anthropogenic emissions into the subtropical jet. To evaluate the significance of convective transport over this region, net (upward minus downward) and gross (upward only) upward mass fluxes across the 500-hPa surface within a domain of 25°–35°N and 110°–120°E were estimated for the entire PEACE-B period based on the ECMWF analyses, and those fluxes were compared with the corresponding upward mass fluxes evaluated only when and where deep convection was identified. Note that for this estimation, we used the analyzed ω-velocity and air density but not convective mass flux derived directly from the convective parameterized scheme in the operational analyses, which is not available in the ECMWF analysis data set. The comparison reveals that 87% of the net upward mass flux and 34% of the gross upward mass flux over central China during the PEACE-B period were associated with deep convection. The latter percentage increases to 52% in another assessment where 500-hPa ω-velocity was used as the sole criterion for identifying convection without using the independent T_{BB} observation data. A part of this increase is considered to be due to errors in the location and/or time of convective activities in the ECMWF analyses; convection was occasionally analyzed by the ECMWF at slightly different locations and/or times than that of actual convective activities, which were detected as high-altitude clouds by the GMS, leading to an underestimation of the frequency of convective activities defined in this study by a coincidence of upward motion and high-altitude clouds. The fact that a significant fraction (34%) of the gross upward mass flux over central China during the period was accounted for by convective activity that occupied only a small fraction (8%) of the entire time period indicates the high efficiency of convective updraft in uplifting air parcels from the PBL into the FT. Furthermore, the ratio between these two quantities (i.e., the mass flux divided by the time fraction) was found rather insensitive to the particular choice of threshold values used for the convection criteria, in spite of the greater sensitivity of the individual quantities, indicating the robustness of our assessment of the significance of convective upward transport.

[22] *Bey et al.* [2001] and *Liu et al.* [2003] showed that episodic frontal uplifting (largely due to WCBs) over central and eastern China caused an upward flux of CO into the lower FT during the PEM-West B (February through the first half of March) and TRACE-P (late February through the beginning of April) periods. The locations where the upward anthropogenic CO fluxes were large at the 3-km level in those periods (see *Bey et al.* [2001, Figure 8a] and *Liu et al.* [2003, Figure 10]) generally agree with the location where the mean 500-hPa ascent was strong (Figure 2c) during the PEACE-B (10 April to 20 May) period, although the relative importance of upward transport mechanisms were different between the PEACE-B and two earlier missions. In the course of the seasonal march, the contribution of convective activity organized in this region

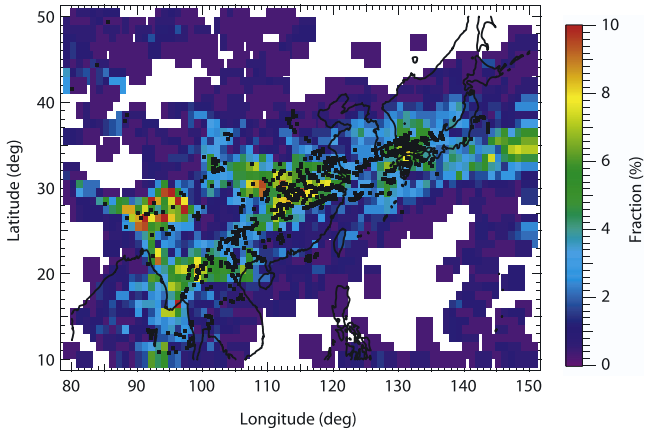

Figure 7. Occurrence probability (time fraction) of convective activity in each 1° × 1° grid box defined in this study for the PEACE-B period (color-coded). Black squares denote locations of convection-hit points (grid boxes in which convective activity was identified when the trajectory of an air parcel passed) of trajectories for air parcels sampled between 4 and 13 km during the PEACE-B period.

to the uplifting of air masses increases substantially by the time of the PEACE-B mission.

3.3. Temporal Variation of Convective Activities

[23] In this section, temporal variations of convective activity over central China during the PEACE-B period are examined in relation to variations in other meteorological variables. Figure 8 shows a time-latitude cross section of 500-hPa ω-velocity averaged between 100°E and 120°E. The midtropospheric updraft over central China (between 25°N and 35°N) was enhanced occasionally (4–5 times) for a few days during the PEACE-B period, namely around 16–18 and 22–25 April and 3–6, 8–9, and 12–14 May, at intervals of 6.5 days on average. As shown below (see Figure 9), convective activity over the region was enhanced on each of these occasions. The pronounced updraft observed on these occasions (in total 16 days), as a whole, contributed largely to the mean upward velocity shown in Figure 2c. This result indicates that the vertical transport of air parcels over central China resulted mainly from a limited number of episodes, rather than through a steady, continuous ascent, in agreement with the results presented in previous studies [*Yienger et al.*, 2000; *Bey et al.*, 2001; *Liu et al.*, 2003; *Jaffe et al.*, 1999; *Wild and Akimoto*, 2001].

[24] Solid lines in Figure 8 indicate latitudes at which the θ_e (equivalent potential temperature) difference between the 500- and 925-hPa levels ($\Delta\theta_e$) became zero, based on the averages for the 100°–120°E longitudinal sector. Roughly speaking, the lines separate dry, cool midlatitude air with stable stratification ($\Delta\theta_e > 0$) from warmer and/or moister subtropical air whose stratification is less stable ($\Delta\theta_e < 0$) and thus favorable for moist convection. We may categorize episodic poleward extensions of subtropical air and corresponding updrafts observed during the PEACE-B period into two types. The first category includes two April episodes of sporadic updraft enhancement over central

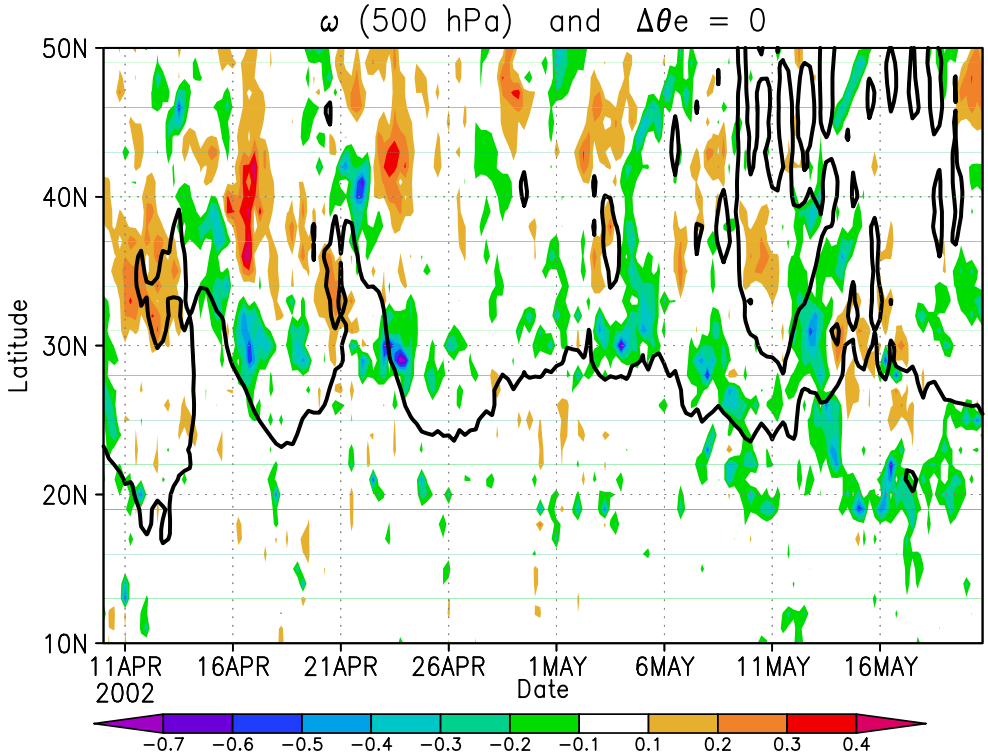

Figure 8. Time-latitude cross section of the 500-hPa ω-velocity averaged longitudinally between 100°E and 120°E (Pa s^{-1}, filled contours) during the PEACE-B period. The black thick lines denote locations where the difference in equivalent potential temperatures between the 500-hPa and 925-hPa levels was zero ($\Delta\theta_e = 0$). The negative $\Delta\theta_e$ region, which corresponds to a convectively unstable region, extended north to 30°–35°N, in association with the intrusions of the warm, moist low-level southerlies.

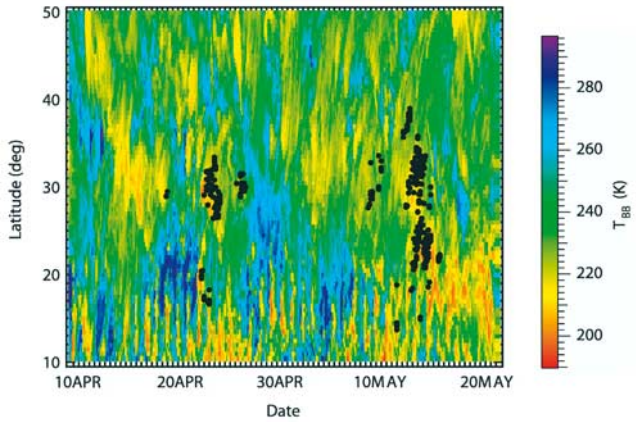

Figure 9. Time-latitude section of the average of the lowest 5% of T_{BB} values observed by the GMS between 100°E and 120°E during the PEACE-B period, as an indicator of the cloud top altitudes of the deepest convective clouds (color-coded). Solid circles denote latitudes and times of convection-hit events that have been identified at any longitude between 100°E and 120°E for air parcels sampled during the PEACE-B mission.

China (days 16–18 and 22–25), each of which occurred immediately after the poleward extension of subtropical air with negative $\Delta\theta_e$ values to ~35°N. Likewise, a domain of negative $\Delta\theta_e$ extended as far north as 40°N right before the mid-May episode (12–14 May) of the markedly enhanced updraft. This episode corresponds to the particular situation discussed in section 3.1 (the case study for CO enhancements observed during flight 10), where the intrusion of the low-level warm, moist southerlies probably contributed substantially to the effective upward transport of pollutants over central China. These episodes in the first category were probably triggered by the passage of migratory cyclonic disturbances. Although the disturbances had relatively small zonal scales and persisted only a few days over the region, their structure was suited for effectively inducing the low-level southerlies and strong updraft as observed. Though less pronounced than in the aforementioned episodes, the second category is represented by a persistent episode of poleward extension (up to ~30°N) of subtropical air ($\Delta\theta_e < 0$) observed between 28 April and 7 May, which appeared to be related to enhanced updraft in early May (days 3–6). Anomalies in 500-hPa height suggest that the persistent episode was associated with the intensified subtropical jet probably due to quasi-stationary Rossby waves. Height anomalies associated with stationary Rossby waves have relatively large zonal scales and equivalent barotropic structure (decreasing amplitude with decreasing altitude). As a consequence, their structure is not particularly suited for effectively inducing southerlies near the surface, although subtropical air ($\Delta\theta_e < 0$) still reached up to ~30°N, as described above (Figure 8). It is noted that a convection episode occurred only once, for a limited time period (for 4 days), within the quasi-stationary Rossby wave period that lasted for 10 days, suggesting that meteorological conditions associated with the Rossby waves by themselves were not sufficient for inducing deep convection in this particular case. Further analysis of the anomalous near-surface southerlies suggests that a trigger of deep convection was likely a migratory cyclonic disturbance for this early May (days 3–6) episode. Though relatively weak, the migratory cyclone could act as an effective trigger for convection in the presence of persistent ascent along the frontal zone and low-level moist southerlies converging into the zone associated with the Rossby waves.

[25] We would like to point out an additional role of the low-level southerlies associated with the migratory cyclonic disturbances or with quasi-stationary Rossby waves. Within the PBL, the southerlies could advect pollutants emitted over south China and Southeast Asian countries effectively into the frontal zone. The low-level wind system is considered to play an important role in controlling the chemical characteristics of air parcels that are finally exported toward the Pacific after convective uplifting.

[26] Figure 9 shows a time-latitude cross section of the average of the lowest 5% of the T_{BB} values between 100°E and 120°E observed by the GMS, as an indicator of cloud top altitudes of the deepest convective clouds in this longitudinal sector. High-altitude clouds with T_{BB} lower than 220 K (above about 10 km) were occasionally seen between 20°N and 40°N. Latitudes and times of those high-altitude cloud events are in general agreement with those of the strong upward motion shown in Figure 8. As described in section 3.2, we identified convection events based on criteria including large negative ω-velocity at 500 hPa and low T_{BB}. The agreement between these two parameters in space and time (Figures 8 and 9) ensures that the high-altitude cloud events, which lasted for a few days between 20°N and 40°N, were due to deep convection.

[27] The vertical cross section of trajectories calculated for air parcels sampled during the PEACE-B mission (Figure 3b) suggests that in addition to convective transport, quasi-adiabatic airstreams along the subtropical jet acted as another vertical transport mechanism over east Asia. Temporal variations of the horizontal wind and θ at the 700-hPa level along the subtropical jet indicate that quasi-adiabatic (nonconvective) ascent over central China intensified ahead of each of the migratory cyclonic disturbances (not shown), suggesting the development of a WCB airstream simultaneously with enhanced convective activity of the first category of convection episodes described above. On the other hand, migratory cyclonic disturbances were rather weak between 28 April and 7 May, when modest enhancement of convective activity likely due to quasi-stationary Rossby waves (the second category of episodes) was occasionally seen. Although slopes of isentropic surfaces along the subtropical jet were relaxed because of the equivalent barotropic structure of the stationary Rossby waves, intensification of the jet possibly retained the strength of the associated quasi-adiabatic ascent slightly above the average.

[28] Our trajectory analysis suggests that air parcels transported by those two processes (i.e., convection and quasi-adiabatic ascent) could occur simultaneously, and polluted air parcels could experience the two processes in sequence. Suppose polluted air parcels near the surface are uplifted by convection. Some of them that detrained at midtropospheric levels would be advected downstream rapidly by the jet stream, while others detrained at upper tropospheric levels would be advected more rapidly by the

stronger westerlies, causing a vertically tilted distribution of the polluted air parcels along the jet. Meanwhile, it would take longer for near-surface air parcels transported by a WCB to reach the same levels because of slower air motion in the lower troposphere. Consequently, pollutants would start spreading vertically and horizontally even if they were uplifted simultaneously from the PBL around the frontal zone over central China on the passage of a single cyclonic disturbance.

3.4. Convection Events Influencing Sampled Air Parcels

[29] To evaluate the influence of deep convection on air parcels sampled from the G-II research aircraft during the PEACE-B period, a 5-day back trajectory was calculated for each of the air parcels sampled every minute at altitudes between 4 and 13 km. By checking the occurrence of convection in each grid box ($1^\circ \times 1^\circ$) every 3 hours along each of the trajectories, we extracted every case in which a trajectory had passed through a convection grid box at an altitude between the top of the PBL (assumed to be at 800 hPa) and the cloud top as inferred from T_{BB}. This procedure is similar to that described by *Koike et al.* [2003a]. Each of the extracted cases is referred to as a "convection-hit event." We recorded all the convection-hit events, even when a back trajectory underwent multiple convection-hit events, and the locations of all of these events were then used to identify the source regions of the sampled air parcels for the analyses described later in section 3.6. The allowance of multiple-hit events for a single trajectory was due to the following reason. In general, for an air parcel that has undergone convective uplifting, a back trajectory extending upstream of the convection event is considered to be unreliable. However, because the typical horizontal scale of individual convection cells is only 20 km or less, an air parcel may not have actually been influenced by convection, even when its trajectory passed through a convection grid box identified in our analysis with the $1^\circ \times 1^\circ$ ($\sim$100 $\times$ 100-km) data. Considering also the uncertainties in trajectory calculations, sampled air parcels had a chance to be influenced by convection at all of the convection-hit points along the trajectory. The average number of hit events is 2.1 for back trajectories that encountered at least one convection-hit event. A spread of multiple convection-hit points, if existing along a trajectory, would represent the uncertainty in the location where the particular air parcel actually departed from the PBL.

[30] Locations of the convection-hit points for all of the air parcels sampled between 4 and 13 km in altitude during the PEACE-B period are plotted in Figure 7 with solid squares. In general, the convection-hit points are located along the subtropical jet (Figure 2d) and concentrated in regions where convective updrafts were frequently identified, namely western Japan, central China (the frontal zone), and Southeast Asia. By simply counting the number of air parcel trajectories, 27% of the sampled air parcels (4–13 km) were found to be influenced by convection. Note that the aircraft measurements were generally carried out at locations and times that chemical transport models had predicted a high possibility of sampling polluted air, especially in the FT. Therefore this percentage (27%) may be statistically biased toward an overestimation of influences from surface sources. Nevertheless, this percentage indicates the significance of convective upward transport, which can affect chemical characteristics of air in the FT.

[31] As an alternative approach to searching for the origin of the sampled air parcels, we also examined the geographical locations where the back trajectories crossed the 800-hPa surface (not shown). In this technique we relied solely on the trajectory calculations, without using any information about convection. In general, the locations of the 800-hPa crossing points are in reasonable agreement with those of the convection-hit points, suggesting the robustness of the air mass origins inferred from our convection-hit analysis. The 800-hPa crossing points are generally located slightly to the southwest of the convection-hit points, because after crossing the 800-hPa level, an ascending air parcel tended to travel slightly northeastward because of the southwesterlies until it encountered a convection grid box. Among the parcels whose trajectories had originated from below the 800-hPa level, 69% were found to be uplifted by convection, indicating the significance of convective activity in uplifting air parcels sampled by the PEACE-B research aircraft.

[32] In Figure 9, a time-latitude distribution of convection-hit events identified at longitudes between 100°E and 120°E is shown for air parcels sampled during the PEACE-B period (closed circles). In this figure, these events are overlaid with the time-latitude cross section of the average of the lowest 5% of T_{BB} values, as discussed in section 3.3. The figure indicates that most of the sampled air parcels affected by convective transport were influenced by major convection events occurring between 20°N and 35°N, especially over China. The chemical characteristics of these sampled air parcels are thus considered to generally represent those of air parcels transported vertically over central China during the PEACE-B period.

3.5. Comparison With Results From Lagrangian Definitions of Convection

[33] In contrast to the present approach in which non-trajectory-based Eulerian criteria were adopted to identify deep convection, as described in section 3.2, trajectory-based Lagrangian approaches have been used in previous studies to identify air parcels that had experienced convective transport processes. *Maloney et al.* [2001] used temporal changes in potential temperature (θ) along trajectories to discriminate convective and nonconvective trajectories for air parcels sampled during NASA's second Pacific Exploratory Mission in the Tropics (PEM-T-B), which was conducted over the tropical Pacific Basin during February through April 1999. They categorized trajectories as convective when two thirds of the trajectory clusters experienced changes in θ greater than 12 K within a 24-hour period (determined using the ECMWF data with a resolution of $1.5^\circ \times 1.5^\circ$) and when the trajectories passed through satellite-observed convection on the day of their largest θ changes. As shown in Figure 3b, air parcels sampled during PEACE-B tend to exhibit large changes in θ along their trajectories when uplifted rapidly in the frontal zone. Among all of the trajectories identified as influenced by convection using our criteria, 71% were categorized as convective based upon the criterion of temporal θ changes along the trajectories adopted by *Maloney et al.* [2001].

Conversely, 69% of the trajectories categorized as convective based only on Maloney et al.'s criterion of θ changes were identified as convective by our criteria, indicating a certain level of consistency between our criteria and those of Maloney et al.

[34] *Miyazaki et al.* [2003] classified uplifted air parcel trajectories sampled during TRACE-P (over the western Pacific in February through April 2001) into WCB, convective, and other categories, based on satellite cloud images and the positions of the trajectories relative to nearby surface cold fronts. For each of the three categories, they estimated the mean ascent rate of air parcels from the altitude changes along their trajectories (from the PBL top to the peak altitudes of the trajectories) divided by their transport time. They obtained 4.7 ± 2.5 and 2.3 ± 1.1 km/24 hours as the mean ascent rates for convective and WCB transport processes, respectively. Obviously, actual updraft velocities of air parcels in the convection core are considered to be much higher than those calculated on the basis of the ECMWF analyses. Nevertheless, the substantially larger grid-scale ascent rate in convective grid boxes than in nonconvective ones reflects the effects of mesoscale convective updrafts, and therefore the grid-scale ascent rates can be used for discriminating between those two vertical transport processes (see discussion in section 3.1). Meanwhile, the mean ascent rate calculated for all the "convection-hit" trajectories identified in this study turns out to be 4.3 ± 2.7 km/24 hours. The good agreement between our results and the corresponding results by *Miyazaki et al.* [2003] indicates the efficacy of our Eulerian-type identification of convective transport.

3.6. Chemical Characteristics of Transported Air Masses

[35] The convection-hit points identified in this study (Figure 7) suggest that sampled air parcels were influenced by PBL air at each of several particular locations along the subtropical jet. In this section, chemical characteristics of these air parcels are described.

[36] The emission inventories of anthropogenic CO over east and Southeast Asia in the year 2000 is shown in Figure 10 [*Streets et al.*, 2003]. High-CO emission regions are located in the northeastern part of China, Japan, and the Republic of Korea (South Korea). The distribution of hot spots (i.e., active fires) detected by a spaceborne Moderate Resolution Imaging Spectroradiometer (MODIS) during the PEACE-B period shows that most were located in Southeast Asia during April and May 2002; however, peak biomass burning activity was evident in March, and the number of hot spots rapidly decreased from early April to later in the month (not shown). As a consequence, the importance of biomass burning emissions over Southeast Asia was not particularly large during the PEACE-B period.

[37] The locations of the individual convection-hit points for air parcels sampled at altitudes between 4 and 13 km are shown in Figures 11a–11d. In these figures, mixing ratios of CO (1-min average), Halon 1211 (CF_2ClBr), tetrachloroethene (C_2Cl_4), and methyl chloride (CH_3Cl) observed on board the aircraft are used for color-coding. For statistical analyses, we defined source regions as shown in Figure 11a, namely, Japan, China, and Southeast Asia, and we call them "Japanese" air masses, etc., hereafter. In Table 1, the median values and the central 67% ranges of mixing ratios of the four chemical species are shown for the three source regions. For comparison, the corresponding median values are shown for "free tropospheric" air parcels that did not experience convective uplifting and remained above the 800-hPa level within the last 5 days prior to the measurement. Of course, no data for "free tropospheric" air parcels are plotted in Figures 11a–11d.

[38] As evident in Table 1, levels of CO and other species were systematically higher in Chinese, Japanese, and Southeast Asian air masses as compared with "free tropospheric" air masses, indicating that vertical transport of PBL air significantly changed air mass characteristics in the FT. In Chinese air masses, CO values are higher than in other air masses (median value is 194 ppbv, Table 1). These high CO concentrations are likely due to anthropogenic emissions, corresponding to areas with particularly high emission rates in the northeastern part of China (Figure 10). As shown in Figure 11b, relatively high Halon 1211 concentrations were also observed in Chinese air masses. Halon 1211 is considered as a unique tracer for Chinese urban emissions [*Blake et al.*, 2001, 2003; *Koike et al.*, 2003b], because China is currently responsible for about 90% of the world's production of Halon 1211, following regulation by the Montreal Protocol [*Fraser et al.*, 1999]. Because of its long residence time in the atmosphere of 10 to 20 years, the differences among the median values of the Halon 1211 concentration were only ~4–7% of the median values, with partial overlapping of its 67% ranges (Table 1). However, since the precision of our measurements (defined as one standard deviation) is as good as 0.028 parts per trillion by volume (pptv) (or a 0.6% deviation), these differences are well above the experimental error and are therefore significant. Furthermore, the number of data with concentrations greater than 4.5 and 4.6 pptv account for 57 and 37% for Chinese air masses, respectively, but for only 10 and 5% or less for other air masses, indicating that Chinese air masses contained many more air parcels with a clear signature of relatively recent influence from Halon 1211 emissions than other air masses. C_2Cl_4, an industrial solvent and chemical intermediate, is considered a useful indicator of industrial emissions [*Blake et al.*, 2003]. The high C_2Cl_4 concentration observed in Chinese air masses thus also suggest influences from industrial sources (Figure 11c). CH_3Cl is a tracer of biomass burning combustion and biofuel burning, although its sources are not completely characterized, with the possibility of an additional contribution from coal burning over east Asia [*Blake et al.*, 2003]. The relatively high CH_3Cl concentrations measured in Chinese air masses may therefore be due to domestic biofuel and possibly coal burning (Figure 11d). Furthermore, the levels of OCS, which has been found to be a good indicator of anthropogenic emission in China [*Blake et al.*, 2004; *Koike et al.*, 2003b], were also high, likely because of coal burning in China (not shown).

[39] Japanese air masses are characterized by relatively high mixing ratios of CO and C_2Cl_4 and relatively low mixing ratios of CH_3Cl. These results suggest that these air masses were strongly influenced by anthropogenic emissions, such as industrial sources and transportation. Southeast Asian air masses are characterized by a relatively high mixing ratios of CH_3Cl and relatively low mixing

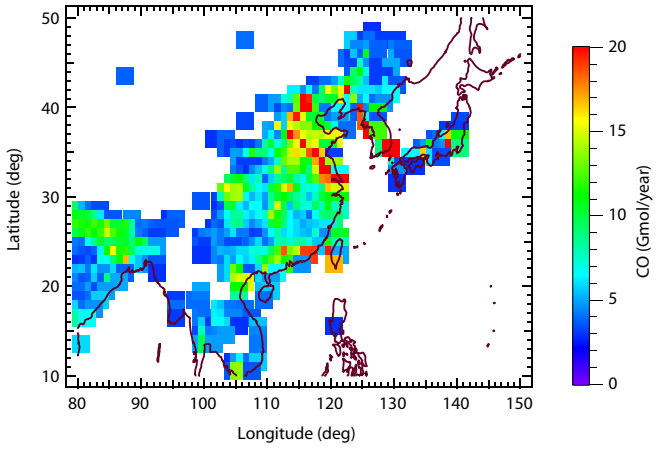

Figure 10. Estimate of anthropogenic CO emissions in the year 2000 at 1° × 1° resolution [*Streets et al.*, 2003]. Only areas in which CO emissions are higher than 3 Gmol/yr are plotted with shading. Note that emissions greater than 20 Gmol/yr are indicated in red.

ratios of C_2Cl_4. As described above, there were some incidents of biomass burning over Southeast Asia, especially in April, which is consistent with the observed relatively high CH_3Cl concentration.

[40] The results presented in this section show that distinct chemical characteristics of uplifted air depend on the locations where they have originated. This demonstrates the importance of a systematic understanding of the location and time of the occurrence of vertical transport processes for evaluating the impact of anthropogenic emissions on regional-to-intercontinental scales. At the same time, the reasonable results (e.g., high Halon 1211 concentrations in Chinese air) indicate the validity of our analyses in which convection-hit points were used to identify the origins of individual air parcels.

4. Comparison of Meteorological Conditions and Uplifting Processes Between the PEACE-A and -B Periods

[41] Mean meteorological fields during the PEACE-A period (6–23 January 2002) are shown in Figures 12a–12d. The low-level circulation was characterized by the prevailing northwesterly flow in association with the Siberian high (Figure 12a), and thus moisture transport over China was much weaker than in the PEACE-B period (Figure 12b). Consistent with the planetary vorticity transport by this northwesterly flow, persistent midtropospheric subsidence was evident over northern China (Figure 12c). In the upper troposphere, an intense subtropical jet was

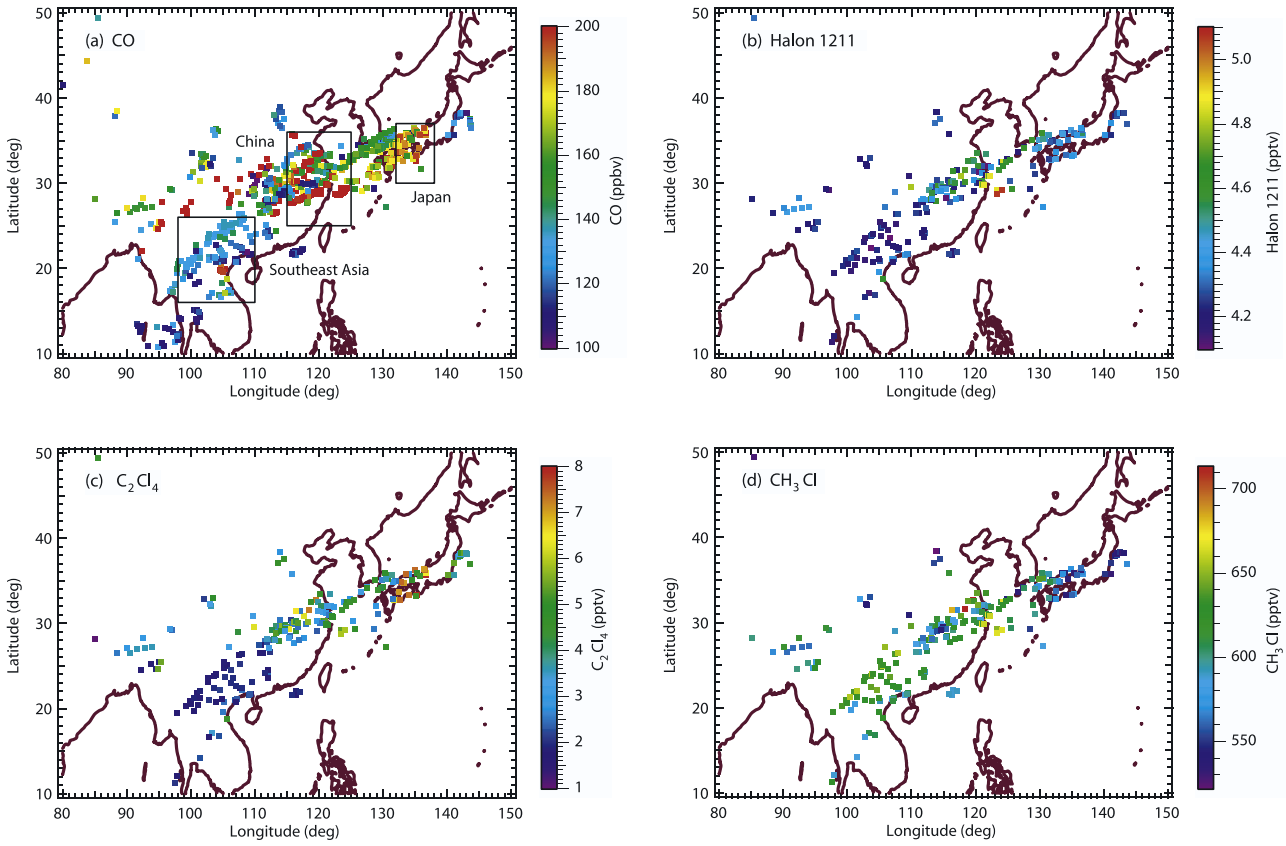

Figure 11. Locations of convection-hit points for all of the air parcels sampled between 4 and 13 km during the PEACE-B period (the same as the black squares shown in Figure 7). The mixing ratios of (a) CO, (b) Halon 1211, (c) C_2Cl_4, and (d) CH_3Cl in individual air parcels sampled on board the aircraft are color-coded. Three primary source regions of the sampled air parcels used for statistical analyses in this study are also shown in Figure 11a. Note that CO concentrations greater than 200 ppbv are indicated in red in Figure 11a.

Table 1. Median Values and Central 67% Ranges of Various Species[a]

Classification	Number of Data[b]	CO, ppbv	Halon 1211, pptv	C_2Cl_4, pptv	CH_3Cl, pptv
Chinese	140	194 (138–215)	4.52 (4.23–4.79)	4.11 (2.56–5.53)	626 (592–662)
Japanese	32	182 (157–192)	4.36 (4.23–4.44)	5.86 (2.64–7.39)	562 (535–572)
Southeast Asian	69	131 (108–141)	4.24 (4.15–4.32)	2.02 (1.77–2.51)	624 (597–636)
Free tropospheric	1005	124 (109–163)	4.21 (4.13–4.30)	2.84 (1.37–4.00)	556 (534–601)

[a]Median values of mixing ratios of various chemical species sampled at altitudes between 4 and 13 km. Values in parentheses are the central 67% ranges.
[b]Number of 1-min CO data used for these statistics.

observed over central China and to the south of Japan (Figure 12d) in association with a strong low-level meridional temperature gradient (Figure 12b). As opposed to the situation in the PEACE-B period (Figure 2c), no pronounced mean updraft was evident over east Asia for the PEACE-A period, indicating that local convection contributed little to the vertical transport of pollutants over this region. In fact, using the same criteria as applied to the PEACE-B analyses (section 3.2), we found the occurrence probability (time fraction) of the deep convection during the PEACE-A period was much lower over the Far East (4% at most) than that during the PEACE-B period.

[42] Instead, WCBs associated with migratory synoptic-scale cyclones could act as an efficient transport mechanism during the PEACE-A period. As a measure of the activity of migratory cyclones (and anticyclones), poleward eddy heat transport ($\overline{v'T'}$) at the 850-hPa level was evaluated locally for the PEACE-A and B periods (Figures 13a and 13b, respectively), where v' and T' are instantaneous deviations from the respective 5-day running means at each grid point and the overbar denotes time averaging over each of the periods. Regions of large eddy heat transport are called "storm tracks" [e.g., *Nakamura et al.*, 2002]. Note that cyclones do not necessarily always accompany WCB air streams [*Eckhardt et al.*, 2004]. Also note that "storm tracks" generally correspond to regions where the lower tropospheric poleward air motion associated with WCBs tend to be large, but they do not necessarily correspond to the origins of air parcels transported by WCBs. Rather, their origins are generally found over the warm water pool off the

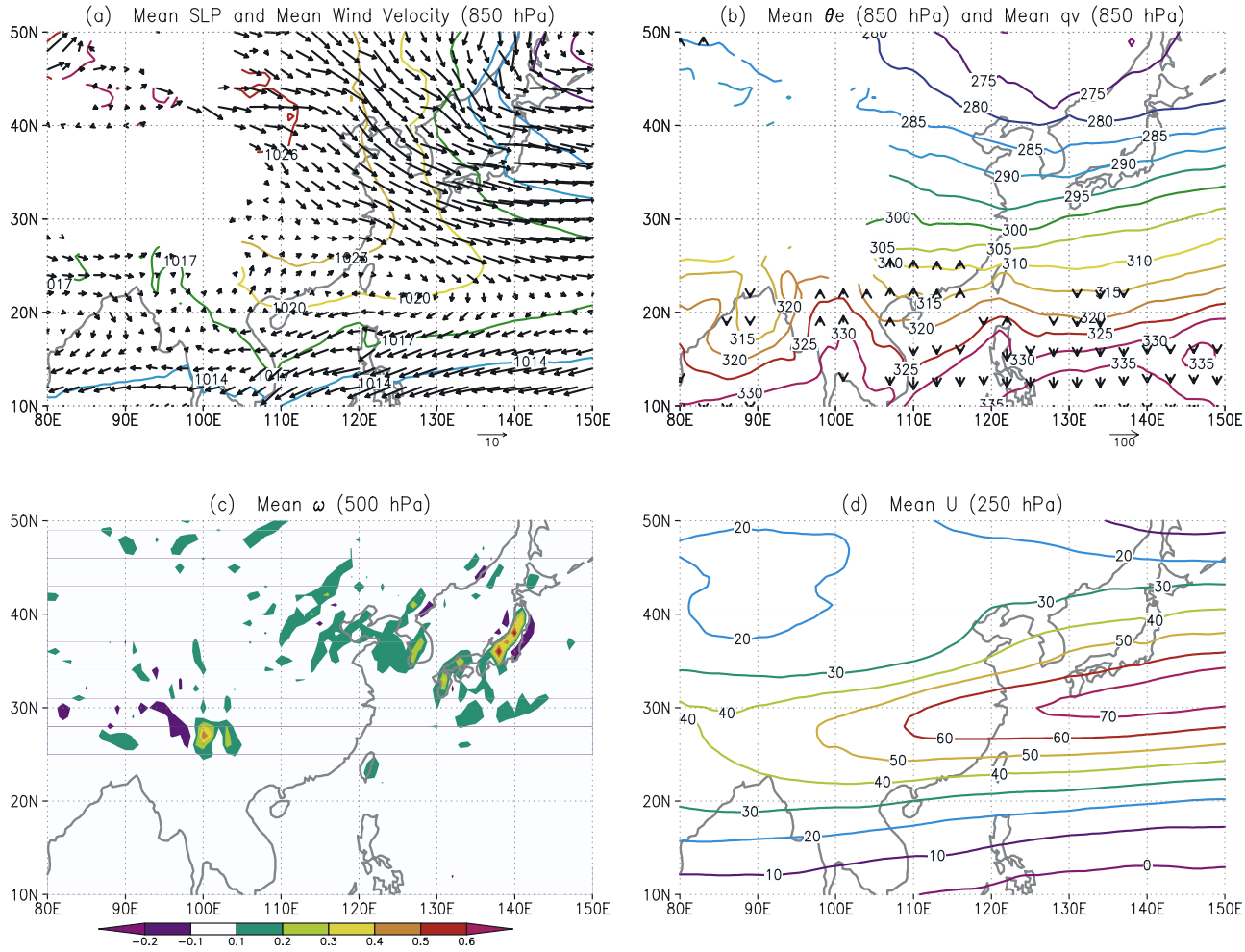

Figure 12. Same as in Figure 2, but for the PEACE-A period (6–23 January 2002).

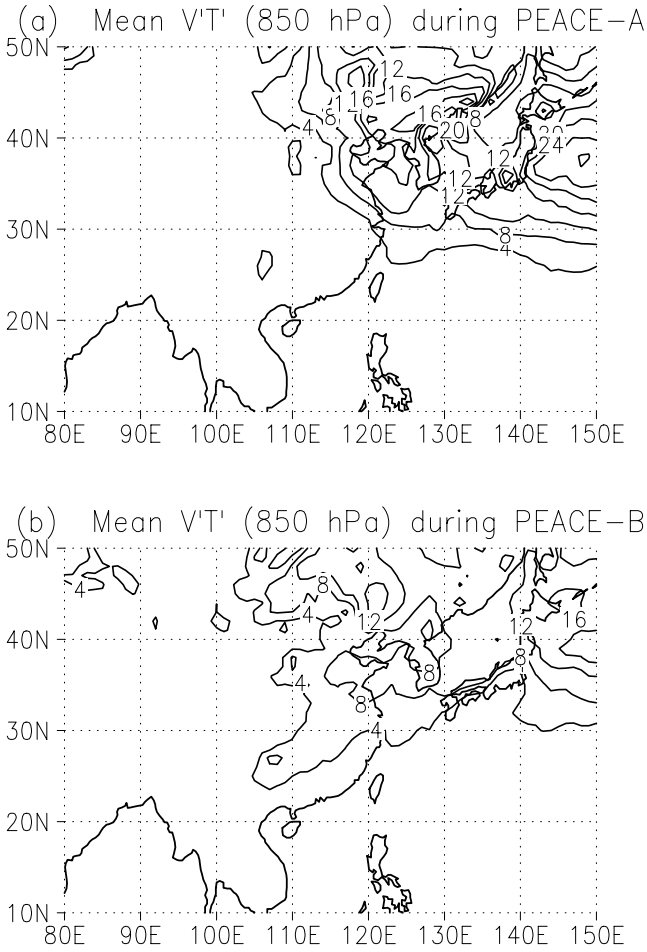

Figure 13. Time-averaged poleward eddy heat transport ($\overline{v'T'}$) at the 850-hPa level (m s^{-1} K) during the (a) PEACE-A and (b) PEACE-B periods, where v' and T' are their instantaneous deviations from their respective 5-day running means at each grid point and the overbar denotes time averaging over each of the periods.

eastern seaboard of Asia between 20°N and 40°N, located upstream of northeastward air motion within the WCB air streams [*Stohl*, 2001; *Eckhardt et al.*, 2004].

[43] During the PEACE-B period, $\overline{v'T'}$ was relatively large over northeastern China (40°–50°N, 110°–125°E, Figure 13b), in association with the northern branch of the double-jet structure (Figure 2d). In that region, the correlation was significantly positive between the two variables (v' and T'), indicating the high activity of baroclinic disturbances (not shown). The eddy heat transport was also large along the Pacific storm track off northeastern Japan. In fact, *Cooper et al.* [2004] made a detailed analysis of intercontinental transport processes for air parcels sampled above the North American west coast during ITCT 2K2, to show that a WCB over the western Pacific was responsible in that case. In contrast, baroclinic transient eddy activity was modest over central China below the subtropical jet, which is consistent with the development of weak cyclonic disturbances in the frontal zone, as discussed in section 3.3.

[44] During the PEACE-A period, migratory cyclone activity was generally higher than that during the PEACE-B period, in association with the stronger meridional temperature gradient and westerly jet (Figures 2 and 12). Correspondingly, vertical transport due to WCBs was much more efficient during the PEACE-A period. This is generally consistent with the trajectory-based WCB analyses by *Stohl* [2001] and *Eckhardt et al.* [2004], who showed that WCBs tend to occur about eight times more frequently in winter than in summer over the North Pacific. We can therefore observe the clear seasonal dependence of the key processes responsible for vertical transport of PBL air into the FT over east Asia. Seasonal warming of the continental surface from winter to summer, with larger warming at higher latitudes, acts to weaken the westerly jet and hence WCB activity, while convective activity is intensified in the subtropical landmass by the time of the PEACE-B mission (late spring). The active convection over southeastern Asia also contributes to the seasonal relaxation of the subtropical jet associated with the weakening of the northern branch of the Hadley circulation.

5. Summary and Conclusions

[45] The PEACE-B aircraft mission was conducted over the western Pacific during April–May 2002. The low-level (850-hPa) circulation during this period was characterized by a persistent southerly flow that advected warm, moist air over south and central China, converging into a quasi-stationary frontal zone along the Yangtze River called the "central China region." Along the frontal zone, a pronounced updraft in the midtroposphere (500 hPa) was seen in the mean field. The mean upper tropospheric circulation was characterized by a double-jet structure over the continent. The surface frontal zone and associated midtropospheric ascent were located below the mean southwesterlies that constituted the subtropical branch of the double-jet. The meteorological conditions over east Asia during the PEACE-B period were found favorable for air masses influenced by anthropogenic emissions over China to be efficiently transported to the FT over the western Pacific.

[46] In this study, criteria to identify deep cumulus convection were developed by combining the ECMWF and GMS data with particular emphasis on the coexistence of strong upward air motion, high-altitude clouds, and sufficient moisture in the lower troposphere. Applying these criteria led to our finding that deep convection frequently occurred along the quasi-stationary frontal zone over central China. The fraction of the time periods in which deep convection observed in central China (25°–35°N and 110°–120°E) was only 8% of the entire PEACE-B period, but those convection events accounted for as much as 34% of the gross upward mass flux across the 500-hPa surface over the entire period. Because the criteria adopted in this study were rather strict, the results indicate the significance of convection as a vertical transport mechanism over central China during the PEACE-B period.

[47] Convective activity over central China intensified on several occasions for a few days at intervals of 4–11 days during the PEACE-B mission, and the vertical transport of air, apparent even in the net mean vertical wind field, resulted mainly from those episodes of enhanced convection. These episodes immediately followed the poleward

extension of subtropical air with conditionally unstable stratification to ~35°N, suggesting that the occasional transport of subtropical moisture by the low-level southerlies into the frontal zone contributed to the enhancement of convective activity. These poleward intrusions of the low-level southerlies occurred in association with either migratory cyclonic disturbances or quasi-stationary Rossby waves. The latter was more persistent but less pronounced, and as a result, pronounced convection occurred only when migratory cyclonic disturbances approached central China.

[48] In contrast to previous studies where trajectory-based Lagrangian approaches were taken to identify air parcels that had experienced convective transport processes [*Maloney et al.*, 2001; *Miyazaki et al.*, 2003], we adopted non-trajectory-based Eulerian criteria to identify convection because of its great computational advantage. In general, a reasonable agreement was found between the outcomes of the two approaches.

[49] To evaluate the influence of deep convection on air parcels sampled from the G-II research aircraft during PEACE-B, we defined "convection-hit" events in which trajectories had passed through convection grid boxes anywhere between the 800-hPa level and the cloud top altitude. By simply counting the number of air trajectories, 27% of the air parcels sampled at altitudes between 4 and 13 km were found to have been influenced by convection. Furthermore, counting the number of trajectories that had originated from the 800-hPa level or below, we found 69% of these air parcels to have been uplifted by convection. Though they may be statistically biased, these values indicate the significance of convective upward transport in determining the chemical characteristics of air in the FT.

[50] Back trajectories of air parcels sampled during the PEACE-B period suggest that a quasi-adiabatic air stream along the subtropical jet also acted as an important vertical transport mechanism, in addition to convective transport. As a migratory cyclonic disturbance approached, the air stream intensified ahead of the cyclone in association with the development of a WCB. Consequently, migratory cyclonic disturbances during the PEACE-B period acted to intensify the two vertical transport mechanisms simultaneously over central China: convection and the quasi-adiabatic air stream (WCB). Air parcels uplifted by these two processes tended to be mixed together around the frontal zone.

[51] The present study also shows that quasi-adiabatic upward transport of air parcels occurred along the quasi-stationary jet axis even without migratory cyclonic disturbances, although it was intensified with a WCB airstream on the passage of the disturbances. These airstreams were weak but persistent and their natures (steady and geographically fixed airstreams) differ from those of classical WCB air streams accompanied by migratory cyclones. The airstreams were primarily due to sloping isentropes along the quasi-stationary jet axis, and they played an important role as another upward transport mechanism of air over central China during PEACE-B.

[52] During several PEACE-B flights, large enhancements of CO greater than 200 ppbv were observed at altitudes between 5 and 10 km. A case study for the highest CO event showed that it was likely due to convective transport of polluted air over central China. Chemical characteristics of convectively uplifted air parcels in various regions were examined by identifying the origins of air parcels by "convection-hit" analysis, and median values of various species were calculated for air masses from China, Japan, and Southeast Asia. In addition, we also examined "free tropospheric" air masses that had neither encountered any convection within the 5 days prior to the measurement nor originated from the 800-hPa level or below. In general, reasonable results were obtained by the present method (e.g., high concentrations of Halon 1211 in Chinese air), indicating the validity of our approach. The results presented in this paper show that vertical transport of PBL air significantly changed the air mass characteristics in the FT. The chemical characteristics of uplifted air masses clearly depended on their locations of origin, demonstrating the importance of a systematic understanding of the locations and times of the vertical transport processes for evaluating the impact of anthropogenic emissions on the atmosphere on regional-to-intercontinental scales. For example, a further increase in anthropogenic emissions in the central China region would likely have a stronger impact on the atmospheric environment in the FT, because of organized upward motion, as compared with other regions in China, at least in late spring. Similarly, the impact of anthropogenic emissions could vary as a result of changes in the locations of frequent upward motion associated with year-to-year variability in meteorological conditions and/or possible regional climate changes in the future. The latter process may result in another complex feedback mechanism for anthropogenic impacts on the atmosphere.

[53] **Acknowledgments.** We are indebted to all of the PEACE-B participants for their cooperation and support. Special thanks are due to the flight and ground crews of the DAS GII aircraft for helping to make this effort a success. The meteorological data were supplied by the European Centre for Medium-Range Weather Forecasts (ECMWF). The trajectory calculation program used in this paper was developed by Y. Tomikawa and K. Sato of the National Institute of Polar Research, Japan. The ITCT 2K2/PEACE campaigns were conducted under the framework of the International Global Atmospheric Chemistry (IGAC) project (http://www.igac.noaa.gov/).

References

Bethan, S., G. Vaughan, C. Gerbig, A. Volz-Thomas, H. Richer, and D. A. Tiddeman (1998), Chemical air mass differences near fronts, *J. Geophys. Res.*, *103*, 13,413–13,434.

Bey, I., D. J. Jacob, J. A. Logan, and R. M. Yantosca (2001), Asian chemical outflow to the Pacific in spring: Origins, pathways, and budgets, *J. Geophys. Res.*, *106*, 23,097–23,113.

Blake, N. J., et al. (2001), Large-scale latitudinal and vertical distribution of NMHCs and selected halocarbons in the troposphere over the Pacific Ocean during the March–April 1999 Pacific Exploratory Mission (PEM-Tropics B), *J. Geophys. Res.*, *106*, 32,627–32,644.

Blake, N. J., et al. (2003), NMHCs and halocarbons in Asian continental outflow during the Transport and Chemical Evolution over the Pacific (TRACE-P) field campaign: Comparison with PEM-West B, *J. Geophys. Res.*, *108*(D20), 8806, doi:10.1029/2002JD003367.

Blake, N. J., et al. (2004), Carbonyl sulfide and carbon disulfide: Large-scale distributions over the western Pacific and emissions from Asia during TRACE-P, *J. Geophys. Res.*, *109*, D15S05, doi:10.1029/2003JD004259.

Browning, K. A. (1990), Organization of clouds and precipitation in extratropical cyclones, in *Extratropical Cyclones: The Erik Palmen Memorial Volume*, edited by C. W. Newton and E. O. Holopainen, pp. 129–153, Am. Meteorol. Soc., Boston, Mass.

Brunner, D., J. Staehelin, and D. Jeker (1998), Large-scale nitrogen oxide plumes in the tropopause region and implications for ozone, *Science*, *282*, 1305–1309.

Carlson, T. N. (1991), *Mid-Latitude Weather Systems*, 507 pp., HarperCollins, New York.

Cooper, O. R., J. L. Moody, D. D. Parrish, M. Trainer, T. B. Ryerson, J. S. Holloway, G. Hübler, F. C. Fehsenfeld, S. J. Oltmans, and M. J. Evans

(2001), Trace gas signatures of the airstreams within North Atlantic cyclones: Case studies from the North Atlantic Regional Experiment (NARE '97) aircraft intensive, *J. Geophys. Res.*, *106*, 5437–5456.

Cooper, O. R., et al. (2004), A case study of transpacific warm conveyor belt transport: Influence of merging airstreams on trace gas import to North America, *J. Geophys. Res.*, *109*, D23S08, doi:10.1029/2003JD003624.

Cotton, W. R., G. D. Alexander, R. Hertenstein, R. L. Walko, R. L. McAnelly, and M. Nicholls (1995), Cloud venting: A review and some new global annual estimates, *Earth Sci. Rev.*, *39*, 169–206.

Dickerson, R. R., et al. (1987), Thunderstorms: An important mechanism in the transport of air pollutants, *Science*, *235*, 460–465.

Donnell, E. A., D. J. Fish, E. M. Dicks, and A. J. Thorpe (2001), Mechanisms for pollutant transport between the boundary layer and the free troposphere, *J. Geophys. Res.*, *106*, 7847–7856.

Dye, J. E., et al. (2000), An overview of the Stratospheric-Tropospheric Experiment: Radiation, Aerosols, and Ozone (STERAO)–Deep Convection experiment with results for the July 10, 1996 storm, *J. Geophys. Res.*, *105*, 10,023–10,045.

Eckhardt, S., A. Stohl, H. Wernli, P. James, C. Forster, and N. Spichtinger (2004), A 15-year climatology of warm conveyer belts, *J. Clim.*, *17*, 218–237.

Esler, J. G., P. H. Haynes, K. S. Law, H. Barjat, K. Dewey, J. Kent, S. Schmitgen, and N. Brough (2003), Transport and mixing between airmasses in cold frontal regions during Dynamics and Chemistry of Frontal Zones (DCFZ), *J. Geophys. Res.*, *108*(D4), 4142, doi:10.1029/2001JD001494.

Fraser, P. J., D. E. Oram, C. E. Reeves, S. A. Penkett, and A. McCulloch (1999), Southern hemispheric halon trends (1978–1998) and global halon emissions, *J. Geophys. Res.*, *104*, 15,985–15,999.

Hannan, J. R., H. E. Fuelberg, J. H. Crawford, G. W. Sachse, and D. R. Blake (2003), Role of wave cyclones in transporting boundary layer air to the free troposphere during the spring 2001 NASA/TRACE-P, *J. Geophys. Res.*, *108*(D20), 8785, doi:10.1029/2002JD003105.

Hov, Ø., and F. Flatøy (1997), Convective redistribution of ozone and oxides of nitrogen in the troposphere over Europe in summer and fall, *J. Atmos. Chem.*, *28*, 319–337.

Jaffe, D., et al. (1999), Transport of Asian air pollution to North America, *Geophys. Res. Lett.*, *26*, 711–714.

Koike, M., et al. (2003a), Reactive nitrogen over the tropical western Pacific: Influence from lightning and biomass burning during BIBLE-A, *J. Geophys. Res.*, *108*(D3), 8403, doi:10.1029/2001JD000823.

Koike, M., et al. (2003b), Export of anthropogenic reactive nitrogen and sulfur compounds from the east Asia region in spring, *J. Geophys. Res.*, *108*(D20), 8789, doi:10.1029/2002JD003284.

Kondo, Y., et al. (2004), Photochemistry of ozone over the western Pacific from winter to spring, *J. Geophys. Res.*, *109*, D23S02, doi:10.1029/2004JD004871.

Kowol-Santen, J., M. Beekmann, S. Schmitgen, and K. Dewey (2001), Tracer analysis of transport from the boundary layer to the free troposphere, *Geophys. Res. Lett.*, *28*, 2907–2910.

Liu, H., D. J. Jacob, I. Bey, R. M. Yantosca, B. N. Duncan, and G. W. Sachse (2003), Transport pathways for Asian combustion outflow over the Pacific: Interannual and seasonal variations, *J. Geophys. Res.*, *108*(D20), 8786, doi:10.1029/2002JD003102.

Maloney, J. C., H. E. Fuelberg, M. A. Avery, J. H. Crawford, D. R. Blake, B. G. Heikes, G. W. Sachse, S. T. Sandholm, H. Singh, and R. W. Talbot (2001), Chemical characteristics of air from different source regions during the second Pacific Exploratory Mission in the Tropics (PEM-Tropics B), *J. Geophys. Res.*, *106*, 32,609–32,625.

Miyazaki, Y., et al. (2003), Synoptic-scale transport of reactive nitrogen over the western Pacific in spring, *J. Geophys. Res.*, *108*(D20), 8788, doi:10.1029/2002JD003248.

Nakamura, H., T. Izumi, and T. Sampe (2002), Interannual and decadal modulations recently observed in the Pacific storm track activity and east Asian winter monsoon, *J. Clim.*, *15*, 1855–1874.

Parrish, D. D., Y. Kondo, O. R. Cooper, C. A. Brock, D. A. Jaffe, M. Trainer, T. Ogawa, G. Hübler, and F. C. Fehsenfeld (2004), Intercontinental Transport and Chemical Transformation 2002 (ITCT 2K2) and Pacific Exploration of Asian Continental Emission (PEACE) experiments: An overview of the 2002 winter and spring intensives, *J. Geophys. Res.*, *109*, D23S01, doi:10.1029/2004JD004980.

Pickering, K. E., A. M. Thompson, J. R. Scala, W.-K. Tao, R. R. Dickerson, and J. Simpson (1992), Free tropospheric ozone production following entrainment of urban plumes into deep convection, *J. Geophys. Res.*, *97*, 17,985–18,000.

Rasch, P. J., N. M. Mahowald, and B. E. Eaton (1997), Representations of transport, convection and the hydrologic cycle in chemical transport models: Implications for the modeling of short-lived and soluble species, *J. Geophys. Res.*, *102*, 28,127–28,138.

Skamarock, W. C., J. G. Powers, M. Barth, J. E. Dye, T. Matejka, D. Bartels, K. Baumann, J. Stith, D. D. Parrish, and G. Hübler (2000), Numerical simulations of the July 10 Stratospheric-Tropospheric Experiment: Radiation, Aerosols, and Ozone/Deep Convection Experiment convective system: Kinematics and transport, *J. Geophys. Res.*, *105*, 19,973–19,990.

Stohl, A. (2001), A 1-year Lagrangian "climatology" of airstreams in the Northern Hemisphere troposphere and lowermost stratosphere, *J. Geophys. Res.*, *106*, 7263–7279.

Stohl, A., and T. Trickl (1999), A textbook example of long-range transport: Simultaneous observation of ozone maxima of stratospheric and North American origin in the free troposphere over Europe, *J. Geophys. Res.*, *104*, 30,445–30,462.

Streets, D. G., et al. (2003), An inventory of gaseous and primary aerosol emissions in Asia in the year 2000, *J. Geophys. Res.*, *108*(D21), 8809, doi:10.1029/2002JD003093.

Wild, O., and H. Akimoto (2001), Intercontinental transport of ozone and its precursors in a three-dimensional global CTM, *J. Geophys. Res.*, *106*, 27,729–27,744.

Xiao, H., G. R. Carmichael, J. Durchenwald, D. Thornton, and A. Bandy (1997), Long-range transport of SO_x and dust in east Asia during the PEM B experiment, *J. Geophys. Res.*, *102*, 28,589–28,612.

Yienger, J. J., et al. (2000), The episodic nature of air pollution transport from Asia to North America, *J. Geophys. Res.*, *105*, 26,931–26,945.

D. R. Blake, Department of Chemistry, University of California, Irvine, Irvine, CA 92697-2025, USA. (drblake@uci.edu)

S. Kawakami and T. Ogawa, Earth Observation Research and Application Center, Japan Aerospace Exploration Agency, 1-8-10 Harumi, Tokyo 104-6023, Japan. (kawakami.shuji@jaxa.jp; ogawa.toshihiro@jaxa.jp)

K. Kita, Department of Environmental Science, Faculty of Science, Ibaraki University, 2-1-1 Bunkyo, Mito, Ibaraki 310-8512, Japan. (kita@env.sci.ibaraki.ac.jp)

M. Koike, H. Nakamura, and N. Oshima, Department of Earth and Planetary Science, Graduate School of Science, University of Tokyo, Hongo 7-3-1, Bunkyo-ku, Tokyo, 113-0033, Japan. (koike@eps.s.u-tokyo.ac.jp; hisashi@eps.s.u-tokyo.ac.jp; oshima@eps.s.u-tokyo.ac.jp)

Y. Kondo, Y. Miyazaki, and N. Takegawa, Research Center for Advanced Science and Technology, University of Tokyo, 4-6-1 Komaba, Meguro, Tokyo 153-8904, Japan. (kondo@atmos.rcast.u-tokyo.ac.jp; yuzom@atmos.rcast.u-tokyo.ac.jp; takegawa@atmos.rcast.u-tokyo.ac.jp)

T. Shirai, National Institute for Environmental Studies, 16-2 Onogawa, Tsukuba, Ibaraki, 305-8506, Japan. (tshirai@nies.go.jp)